Turnbuckle diamond anvil cell for high-pressure measurements in a superconducting quantum interference device magnetometer

AIP | Review of Scientific Instruments

Turnbuckle diamond anvil cell for high-pressure measurements in a superconducting quantum interference device magnetometer

Gaétan Giriat, Weiwei Wang, J. Paul Attfield, Andrew D. Huxley, and Konstantin V. Kamenev

Citation: Rev. Sci. Instrum. **81**, 073905 (2010); doi: 10.1063/1.3465311
View online: http://dx.doi.org/10.1063/1.3465311
View Table of Contents: http://rsi.aip.org/resource/1/RSINAK/v81/i7
Published by the American Institute of Physics.

Turnbuckle diamond anvil cell for high-pressure measurements in a superconducting quantum interference device magnetometer

Gaétan Giriat,[1] Weiwei Wang,[1] J. Paul Attfield,[2] Andrew D. Huxley,[3] and Konstantin V. Kamenev[1,a)]

[1]*Centre for Science at Extreme Conditions and School of Engineering, University of Edinburgh, Edinburgh EH9 3JZ, United Kingdom*

[2]*Centre for Science at Extreme Conditions and School of Chemistry, University of Edinburgh, Edinburgh EH9 3JZ, United Kingdom*

[3]*Centre for Science at Extreme Conditions and School of Physics, University of Edinburgh, Edinburgh EH9 3JZ, United Kingdom*

(Received 26 May 2010; accepted 27 June 2010; published online 27 July 2010)

We have developed a miniature diamond anvil cell for magnetization measurements in a widely used magnetic property measurement system commercial magnetometer built around a superconducting quantum interference device. The design of the pressure cell is based on the turnbuckle principle in which force can be created and maintained by rotating the body of the device while restricting the counterthreaded end-nuts to translational movement. The load on the opposed diamond anvils and the sample between them is generated using a hydraulic press. The load is then locked by rotating the body of the cell with respect to the end-nuts. The dimensions of the pressure cell have been optimized by use of finite element analysis. The cell is approximately a cylinder 7 mm long and 7 mm in diameter and weighs only 1.5 g. Due to its small size the cell thermalizes rapidly. It is capable of achieving pressures in excess of 10 GPa while allowing measurements to be performed with the maximum sensitivity of the magnetometer. The performance of the pressure cell is illustrated by a high pressure magnetic study of $Mn_3[Cr(CN)_6]_2 \cdot xH_2O$ Prussian blue analog up to 10.3 GPa. © *2010 American Institute of Physics.* [doi:10.1063/1.3465311]

I. INTRODUCTION

Magnetization (M) is a fundamental physical property characterizing the response of a material to applied magnetic field. Knowing its temperature (T), field (H), and pressure (P) dependence reveals the nature of magnetic interactions, the value of the exchange parameters, the critical T, H, and P of magnetic phase transitions, etc. While the ability to change temperature and magnetic field comes as standard in commercially available magnetometers, in order to perform high-pressure measurements custom built pressure cells are required. Most existing pressure cells for magnetization measurements have been made for use with the Magnetic Property Measurement System (MPMS®) from Quantum Design (USA)[1] based on a superconductive quantum interference device (SQUID). The MPMS can resolve magnetic moment changes as small as 10^{-8} emu but has the inner bore of only 9 mm diameter which is a major constraint in the design of a pressure cell.

Pressure cells can be divided into two generic categories – piston-cylinder and opposed anvil devices. Most of the pressure cells designed for the MPMS are of piston-cylinder type.[2–9] Relatively large sample volume is one of the key advantages of this design. However, the disadvantage is that the pressure range is limited to approximately 2 GPa. The opposed anvil devices can achieve significantly higher pressures and in the following section we review the existing MPMS pressure cells of this design.

II. EXISTING OPPOSED-ANVIL PRESSURE CELLS FOR MPMS MAGNETOMETERS

Mito *et al.*[10] designed the first diamond anvil cell (DAC) for a SQUID magnetometer. The pressure cell was made of nonmagnetic copper beryllium alloy and depending on the size of the diamond culets was capable of reaching a pressure of 15 GPa. The alignment of the anvils was achieved by adjusting the position of one of the diamonds in the horizontal plane while the other diamond was attached to a hemispherical support, which provided the option for its tilt alignment. Pressure was applied by turning the nut at the back of the piston and thus transmitting the load onto the anvil attached at the opposite end. Since the original publication there have been several modifications of this design.[11–13] A pressure cell of a similar design called Mcell Ultra is commercially available from easyLab Technologies (UK).[7]

A somewhat different design of a SQUID DAC has been proposed by Alireza *et al.*[14,15] The key difference between this and Mito's design is the absence of the rocking support and the tilt alignment. The cell is made of ultrapure BeCu and CuTi alloys and the design is optimized in order to minimize the amount of the cell material around the sample and to provide large windows in order to improve the signal-to-background of the measurement.

a)Electronic mail: k.kamenev@ed.ac.uk.

In a measurement of magnetization, the sample and cell are displaced through a series of superconducting coils separated by a total distance of 4 cm and the change in flux passing through the combination of coils is recorded. In principle a long uniform cell body would not contribute to the signal when it is displaced along its length. The preceding cells all have lengths of many centimeters to approximately achieve this. There are three sources of background signal: (i) changes in cross-section, metal composition, and end corrections mean that a small signal is nevertheless generated from the length of the cell which is not modeled by standard fitting functions used to extract the magnetization from the data. (ii) The construction of the section of the cell adjacent to the sample is necessarily nonuniform and generates a background signal. (iii) Any nonsymmetry around the sample position along the length of the cell makes it difficult to center a weakly magnetic sample accurately in the coils and apply the background correction owing to small displacements of the cell components. Our cell differs from previous designs in being both symmetric around the sample and extremely short, comparable to the size of gelatin capsules used for measuring samples at ambient pressure. This means that all the background magnetization due to the cell is captured by the standard fitting model (or a simple modification thereof) and errors due to component shifts are minimal when subtracting the empty cell signal. We thus avoid background sources (i) and (iii). Furthermore, by using only low susceptibility materials, and minimizing the cell dimensions, the background signal from source (ii) is very low giving excellent sensitivity to the sample magnetization. In the next section we describe the design of such a pressure cell.

III. DESIGN AND OPERATION

The operation of the DAC is based on the turnbuckle principle. Conventionally such devices are used for creating tensile strain and for tightening cables. In high pressure cells the turnbuckle is used for applying compressive force by pushing the counterthreaded parts toward each other inside the body of the device. This idea was first applied to the design of a pressure cell by Tozer and co-workers.[16–18] They developed pressure cells for resistivity measurements, some of which are made of hard plastic material for use in pulsed magnetic fields. A turnbuckle cell for magnetization measurements was also reported in a study of TmTe up to 6.1 GPa,[19] but full details of the cell design and construction were not presented.

The pressure cell we have built for magnetization measurements is made of a fully hardened beryllium-copper alloy (BERYLCO 25) supplied by NGK Berylco (UK),[20] and is abbreviated TM-DAC for "turnbuckle magnetic DAC." The design is shown in Fig. 1. The TM-DAC consists of a body and two end-nuts. The body is a cylinder 7 mm long and 7 mm in diameter with flats made for gripping it when rotating. Four holes have been machined in the sides for viewing the anvils and the gasket. The two end-nuts have four guiding holes drilled in them at the outer end and the diamond anvil attached with Stycast epoxy at the other end.

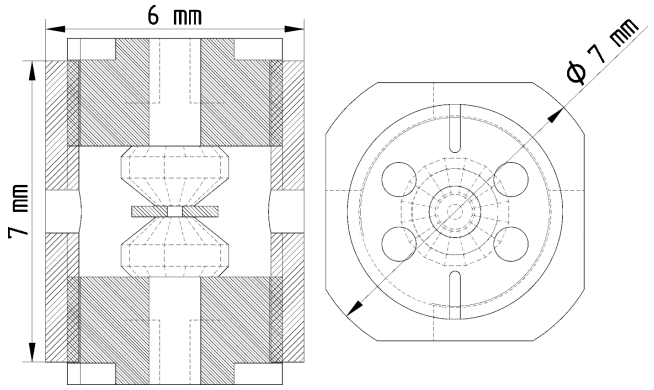

FIG. 1. Drawings of the TM-DAC with key dimensions.

The end-nuts are identical apart from having the external $M5 \times 0.5$ thread cut in opposite directions, i.e., left-hand for the top nut and the right-hand for the bottom one. In order to maximize the strength of the body and to minimize the amount of the cell material around the sample, we modeled the behavior of the cell under load using finite element analysis.[21] The simulations show that the cell can hold loads in excess of 6 kN between the end-nuts.

The parts of the TM-DAC are shown in Fig. 2(a). During the assembly of the pressure cell the diamonds were glued to the end-nuts in such a way that their culets were coaxial with the viewing hole in the nut. There is no alignment mechanism and the anvil alignment is achieved through precision machining of the end-nuts and the body of the pressure cell.

As the gasket material we use annealed BERYLCO 25 foil. The gasket was preindented from 250 to 120 μm and the hole of 350 μm was drilled in it, making the initial sample volume equal to approximately 10^{-2} mm^3. During the tests and measurements discussed in this report, we used diamonds with 800 μm culets to achieve pressures in excess of 10 GPa. With smaller culets higher pressures can be reached though at the cost of having a smaller sample volume.

The sample and the pressure marker were loaded into the hole in the gasket and Daphne 7373 oil was used as the pressure transmitting medium.[22] Depending on the requirements of the experiment the pressure inside the cell could be measured either by ruby fluorescence or by following the critical temperature T_c of a superconducting transition in a reference material with known $T_c(P)$ such as Pb, Sn, or In.[23]

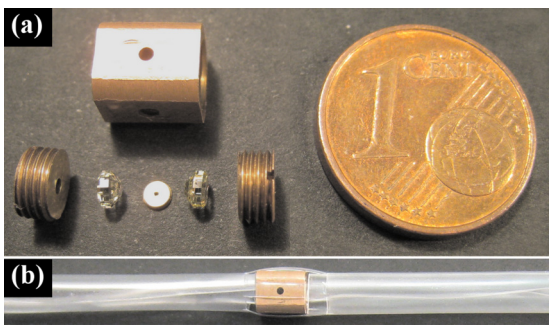

FIG. 2. (Color online) (a) Parts of the TM-DAC. (b) The assembled TM-DAC in the standard plastic straw holder of MPMS.

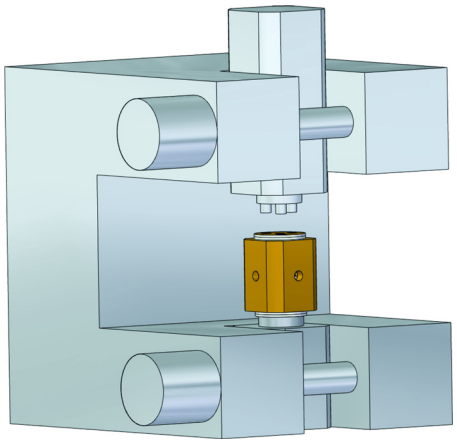

FIG. 3. (Color online) Computer-aided design drawing of the bracket for applying load to the TM-DAC.

Once the sample is loaded, the pressure cell is placed into a specially designed bracket with four pins engaging into the four holes in both end-nuts as shown in Fig. 3. The part of the bracket with the top pins can slide vertically allowing the pressure cell to be put into the bracket and also to adjust the height of the pins to ensure that they engage fully into the guide holes in the end-nuts.

Once the pins are engaged they can only slide up and down when the body of the cell is rotated. While it is possible to generate some initial pressure by turning the body of the cell held inside the bracket, at higher loads the friction on the thread between the body and the end-nuts becomes large. In order to overcome this problem, the bracket is placed into a hydraulic press and the load, monitored by a sensitive load cell, is applied in small steps. This process closes a small gap that appears between the threads of the end-nuts and the body of the cell due to the deformation along the pitch-line contact in the locked turnbuckle. This relaxes the threads which enables the operator to lock the load by turning the body of the cell with respect to the end-nuts. The pressure during this process can also be checked by using ruby fluorescence. Once the desired pressure is achieved the pressure cell is placed in the holder for measurements in the magnetometer. For our measurements we adapted a standard plastic straw recommended for use with the MPMS as shown in Fig. 2(b).

IV. TESTS AND RESULTS

The TM-DAC has been extensively tested and in this section we provide a summary of the test results. We note that because the cell is symmetric with respect to the sample and because it is so short, with dimensions close to those of a standard MPMS sample, the cell produces a symmetric response of the voltage measured through the SQUID element as illustrated in Fig. 4. This remains true for all applied magnetic fields. It also allows the signal from the cell to be measured over the recommended full 6 cm scan and the measurement does not need to be limited to a shorter scan length in order to exclude the interference from the end parts as is the case in longer pressure cells.

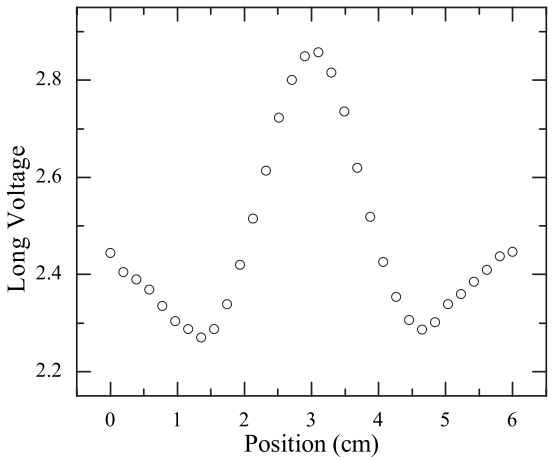

FIG. 4. Raw MPMS data generated by a scan of the empty TM-DAC over a 6 cm distance in an applied field of 20 Oe at 300 K. The resulting integrated magnetization as calculated by the MPMS software is 1.07×10^{-5} emu.

Another advantage of having the cell fully enclosed in the scan range is that the changes in the relative position of the parts of the cell occurring when pressure is changed do not affect the integrated signal. Hence the same background correction can be applied to measurements at all pressures and the observed changes to the signal with pressure originate from the sample. The sensitivity of the MPMS measurements is not affected by the presence of the pressure cell, i.e., the accuracy of the measured signal from a given sample within the cell is the same as from that sample in a standard MPMS gelatin capsule.

The weight of the assembled TM-DAC is approximately 1.5 g. It can therefore be cooled at a high rate and can quickly reach thermal equilibrium. The magnetic signal from the cell measured in several magnetic fields as a function of temperature is presented in Fig. 5. The curves are smooth and follow the known trend for BERYLCO 25 alloy. The magnetization of the empty pressure cell as a function of field and temperature was recorded prior to the measurement with the sample and the data were used for background correction.

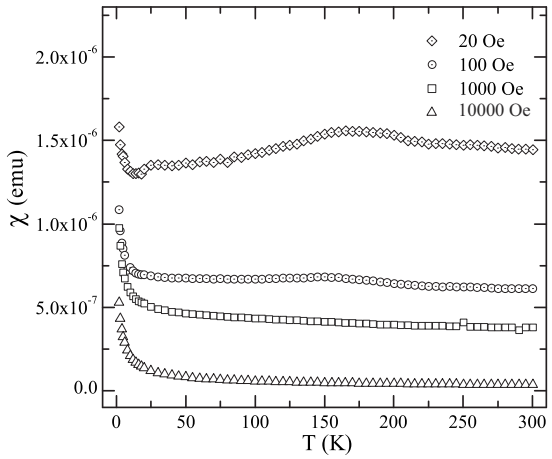

FIG. 5. The temperature dependence of the magnetization of an empty TM-DAC shown as $\chi = M/H$ for different magnetic fields.

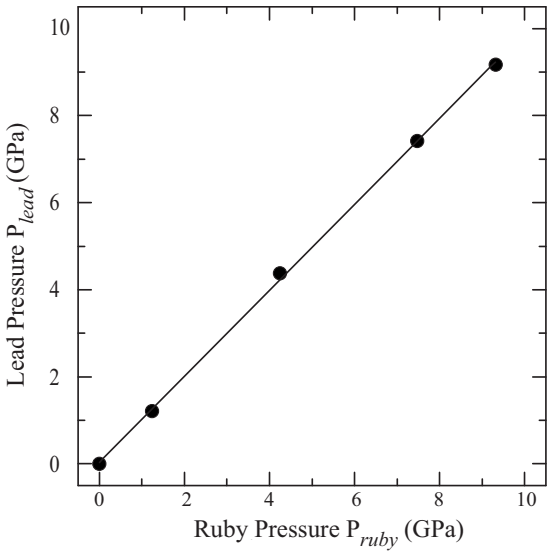

FIG. 6. The pressure P_{lead} determined at the superconducting transition in lead at low temperature ($T \approx 3-7$ K) vs the pressure P_{ruby} derived from the ruby fluorescence at ambient temperature ($T \approx 295$ K). The solid line shows $P_{\text{lead}}=P_{\text{ruby}}$. The errors in determining the pressure are ± 0.03 GPa for lead and ± 0.02 GPa for ruby. The error bars are smaller than the symbols on the graph.

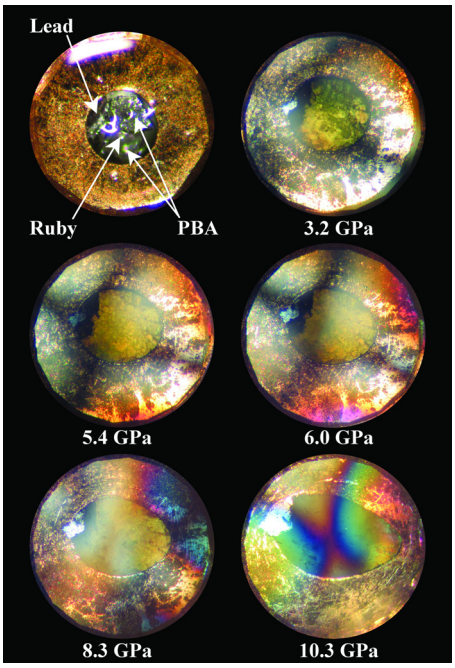

FIG. 7. (Color online) Photographs of the gasket hole taken at several pressure points during loading. The hole contains the sample of $Mn_3[Cr(CN)_6]_2 \cdot xH_2O$ PBA, a speck of Pb, and a ruby chip. The elongation of the sample hole illustrates the quality of the anvil alignment.

In order to establish whether the pressure changes in the TM-DAC on cooling, we performed a test in which ruby and lead were loaded into the sample volume. Ruby fluorescence was used to establish pressure at room temperature while lead was used to measure the pressure at low temperature (3–7 K) by following T_c for the same loading and taking the value of $dT_c/dP=0.365$ K/GPa.[23] It is notable that the pressure remains the same at low temperature as at room temperature, as shown in Fig. 6, so that either of the pressure measurements is sufficient.

V. MAGNETIC PROPERTIES OF A PRUSSIAN BLUE ANALOG UNDER PRESSURE

We illustrate the performance of the TM-DAC through a study of $Mn_3[Cr(CN)_6]_2 \cdot xH_2O$. This ferrimagnet material is a Prussian blue analog (PBA) compound and consists of a cubic network of alternating $Mn(CN)_6$ and $Cr(NC)_6$ octahedra connected through the cyanide bridges. The sample used here has $x \approx 16$ and its preparation, structure, and magnetic properties up to 1 GPa pressure are reported elsewhere.[24] $Mn_3[Cr(CN)_6]_2 \cdot xH_2O$ was loaded into the pressure cell with a ruby chip and a small piece of lead for independent pressure measurement. In Fig. 7 we show photographs of the gasket hole taken through the microscope, which show the sample, ruby, and lead and also illustrate the performance of the gasket at high pressure.

Pressure was applied in small steps after each of which magnetic susceptibility was measured as a function of temperature (Fig. 8). A small feature at $T \sim 60$ K is present in all the data sets and its magnitude and position are not affected by applied pressure. The temperature at which it is observed corresponds to the Curie temperature T_C of the PBA at ambient pressure, and we therefore attribute this feature to a minute amount of the sample left outside the pressurized volume of the cell after loading into the gasket hole.

The sample magnetization M is shown as low-field susceptibility $\chi=M/H$, in an $H=100$ Oe field throughout this section, and with mass susceptibility $\chi_m=\chi/m$, where the sample mass was $m=7.5\times10^{-6}$ g. The pressure variations of T_C, derived from the maximum of $d\chi/dT$, and $\Delta\chi_m = \chi_m(40\text{ K}) - \chi_m(120\text{ K})$, taken as being proportional to the

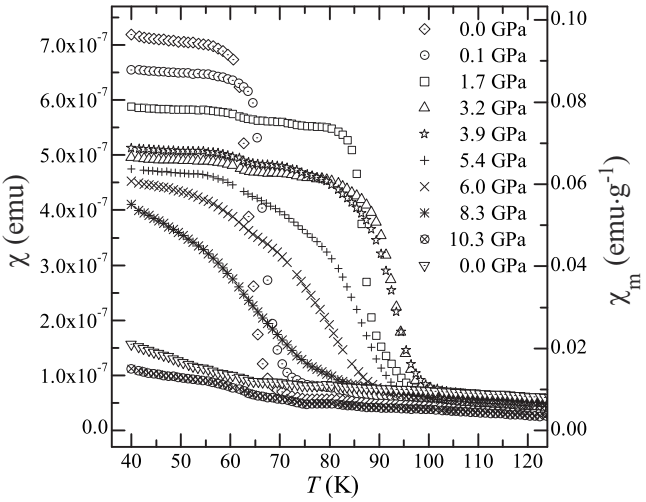

FIG. 8. The temperature dependence of the magnetic susceptibility of $Mn_3[Cr(CN)_6]_2 \cdot xH_2O$ in a 100 Oe field at several pressures. The data have been collected on warming after cooling down in field and are corrected for the cell background. The final (inverted triangle) data are collected after the release of pressure. To illustrate the sensitivity of the measurement the left axis shows the susceptibility χ in emu while the right axis shows χ_m values normalized by the mass of the sample $m=7.5\times10^{-6}$ g, estimated from the comparison of the $\chi(T)$ measurements performed at ambient pressure on the sample in a plastic straw and in the TM-DAC.

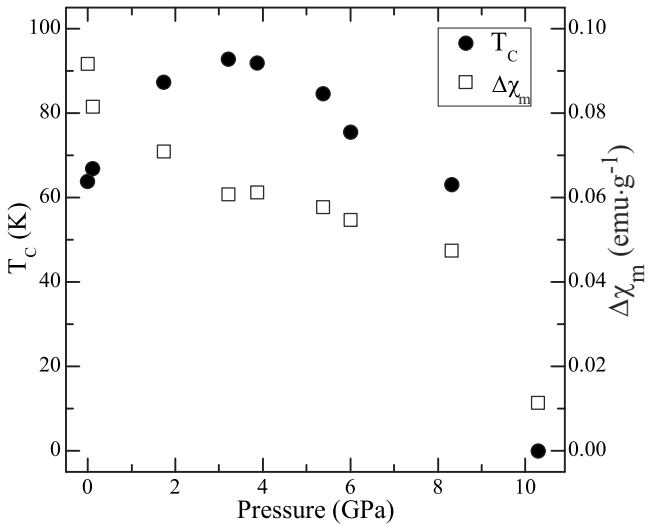

FIG. 9. The pressure-temperature magnetic phase diagram of $Mn_3[Cr(CN)_6]_2 \cdot xH_2O$. $\Delta\chi_m$ shows the difference between the values of mass susceptibility taken at 40 K, χ_m(40 K), and 120 K, χ_m(120 K) (see Fig. 8).

ferrimagnetic moment, are shown in Fig. 9. The initial $dT_C/dP = 25$ K/GPa is similar to the values reported in two previous studies at pressures below 1 GPa.[25,24] At higher pressures, a substantial but nonlinear increase in T_c from 63 K at ambient pressure to a maximum $T_C = 93$ K at 3.2 GPa pressure is discovered. This reflects an enhancement of the superexchange interactions between the transition metal cations as the bonds to cyanide are shortened with pressure. The ferrimagnetic moment decreases as T_C is enhanced which may evidence increased tilting of the $Mn(CN)_6$ and $Cr(NC)_6$ octahedra. At pressures above 3.2 GPa the magnetic transition becomes much broader and T_C is suppressed to zero near 10 GPa, with a corresponding collapse of the ferrimagnetic moment. This is consistent with a pressure-induced amorphization of the sample, as was observed in a similar PBA, $FeCo(CN)_6$ between 8 and 10 GPa.[26] The observation that the ferrimagnetism of $Mn_3[Cr(CN)_6]_2 \cdot xH_2O$ does not recover when the pressure in the pressure cell is released from 10 GPa (see the last zero pressure point in Fig. 8) supports this conclusion but a structural study up to 10 GPa will be needed for confirmation.

VI. CONCLUSIONS

In summary, we have designed, constructed, and tested a miniature turnbuckle DAC for magnetic susceptibility measurements in a commercial SQUID magnetometer. Due to its low thermal mass it can be thermally equilibrated rapidly which helps to save time and cryogenic consumables during the measurements. The pressure cell is capable at maintaining pressures in excess of 10 GPa and allows highly sensitive magnetization measurements to be performed as demonstrated by a study of $Mn_3[Cr(CN)_6]_2 \cdot xH_2O$.

ACKNOWLEDGMENTS

The authors acknowledge support from EPSRC Grant No. EP/E06471X/1 and the Leverhulme Trust.

[1] See: http://www.qdusa.com/ for Quantum Design.
[2] S. Reich and T. Godin, Meas. Sci. Technol. **7**, 1079 (1996).
[3] J. Diederichs, A. K. Gangopadhyay, and J. S. Schilling, Phys. Rev. B **54**, R9662 (1996).
[4] Y. Uwatoko, T. Hotta, E. Matsuoka, H. Mori, T. Oki, J. L. Sarrao, J. D. Thompson, N. Mori, and G. Oomi, Rev. High Pressure Sci. Technol. **7**, 1508 (1998).
[5] K. Kamishima, M. Hagiwara, and H. Yoshida, Rev. Sci. Instrum. **72**, 1472 (2001).
[6] J. Kamarád, Z. Machátová, and Z. Arnold, Rev. Sci. Instrum. **75**, 5022 (2004).
[7] See: http://www.easylab.co.uk/ for Mcell 10 and Mcell Ultra pressure cells manufactured by easyLab Technologies.
[8] K. V. Kamenev, S. Tancharakorn, N. Robertson, and A. Harrison, Rev. Sci. Instrum. **77**, 073905 (2006).
[9] Y. Uwatoko, T. Fujiwara, M. Hedo, F. Tomioka, and I. Umehara, J. Phys.: Condens. Matter **17**, S1011 (2005).
[10] M. Mito, M. Hitaka, T. Kawae, K. Takeda, T. Kitai, and N. Toyoshima, Jpn. J. Appl. Phys., Part 1 **40**, 6641 (2001).
[11] M. Mito, J. Phys. Soc. Jpn. **76**, 182 (2007).
[12] S. Tominaga, Y. Komorida, M. Mito, H. Deguchi, S. Takagi, K. Koyama, and M. Hamada, J. Phys.: Conf. Ser. **150**, 052271 (2009).
[13] T. C. Kobayashi, H. Hidaka, H. Kotegawa, K. Fujiwara, and M. I. Eremets, Rev. Sci. Instrum. **78**, 023909 (2007).
[14] P. L. Alireza, S. Barakat, A.-M. Cumberlidge, G. Lonzarich, F. Nakamura, and Y. Maeno, J. Phys. Soc. Jpn. **76**, 216 (2007).
[15] P. L. Alireza and G. G. Lonzarich, Rev. Sci. Instrum. **80**, 023906 (2009).
[16] M. Kano, N. Kurita, M. Hedo, Y. Uwatoko, S. W. Tozer, H. S. Suzuki, T. Onimaru, and T. Sakakibara, J. Phys. Soc. Jpn. **76**, 56 (2007).
[17] W. A. Bassett, High Press. Res. **29**, 163 (2009).
[18] C. Martin, C. C. Agosta, S. W. Tozer, H. A. Radovan, T. Kinoshota, and M. Tokumoto, J. Low Temp. Phys. **138**, 1025 (2005).
[19] L. Chen, N. Kurita, M. Hedo, K. Nakazawa, I. Oguro, Y. Uwatoko, T. Matsumura, M. Tokumoto, and S. W. Tozer, J. Phys. Soc. Jpn. **76**, 58 (2007).
[20] See: http://www.ngkberylco.co.uk/ for NGK Berylco U.K. Ltd.
[21] See: http://www.ansys.com/ for ANSYS, Inc.
[22] K. Murata, H. Yoshino, H. O. Yadav, Y. Honda, and N. Shirakawa, Rev. Sci. Instrum. **68**, 2490 (1997).
[23] A. Eiling and J. S. Schilling, J. Phys. F: Met. Phys. **11**, 623 (1981).
[24] G. Giriat, A. Harrison, D. R. Allan, K. V. Kamenev, and D. S. Middlemiss, "Tuning magnetic superexchange in a Prussian Blue Analogue with pressure," Phys. Rev. B (to be published).
[25] M. Zentková, Z. Arnold, J. Kamarád, V. Kavečanský, M. Lukáčová, S. Mat'aš, M. Mihalik, Z. Mitróová, and A. Zentko, J. Phys.: Condens. Matter **19**, 266217 (2007).
[26] J. Catafesta, J. Haines, J. E. Zorzi, A. S. Pereira, and C. A. Perottoni, Phys. Rev. B **77**, 064104 (2008).